Fibers and Polymers 2018, Vol.19, No.2, 403-415
DOI 10.1007/s12221-018-7759-6

ISSN 1229-9197 (print version)
ISSN 1875-0052 (electronic version)

An Investigation on Wear and Dynamic Mechanical behavior of Jute/Hemp/Flax Reinforced Composites and Its Hybrids for Tribological Applications

Vijay Chaudhary*, Pramendra Kumar Bajpai, and Sachin Maheshwari

Division of Manufacturing Process and Automation Engineering, Netaji Subhas Institute of Technology, University of Delhi, Delhi 110078, India

(Received September 3, 2017; Revised November 29, 2017; Accepted December 2, 2017)

Abstract: Bio-materials have ignited a quest among research fraternity to be used in every possible field of applications like automobile, sports, medical, civil and textile industry. Application spectrum of natural fiber reinforced polymer composites is spreading globally in every field of engineering having structural and tribological applications. The present work investigates the tribological performance of regionally available inexpensive plant based natural fiber reinforced polymer composites. In this work, three different types of natural fibers (jute, hemp, and flax) were reinforced with epoxy matrix to fabricate natural fiber reinforced polymer composites (NFRP) and their hybrid composites (jute/hemp/Epoxy, hemp/flax/epoxy and jute/ hemp/flax/epoxy) using hand-layup technique. Tribological performance of the developed bio-composites were evaluated in terms of frictional characteristics and sliding wear under dry contact condition at different process parameters, such as applied load (10-50 N), sliding speed (1-5 m/s) and sliding distance (1000-2000 m). Experimental results of wear analysis confirmed that incorporation of natural fibers into epoxy polymer matrix significantly improved the wear behavior of the developed NFRP composites in comparison to neat epoxy polymer. Among all the developed composites, jute/epoxy composite achieved the highest coefficient of friction, frictional force and specific wear rate. Dynamic mechanical analysis (DMA) was also analyzed to evaluate the viscoelastic behavior of the developed composites. The surface morphology of samples after wear test was examined by scanning electron microscopy to investigate and propose the possible wear mechanism of the developed composites.

Keywords: Sliding wear, Sliding friction, DMA, Natural fiber, Epoxy, SEM

Introduction

The increased environmental consciousness is promoting the use of eco-friendly fibers, extracted from plants, vegetables, minerals and animals instead of synthetic fibers [1]. Various properties of natural fibers such as light weight, high specific strength, good wear resistance and non-toxicity makes it easier to replace the synthetic fibers as well as conventional metallic materials. Due to these massive properties, natural fibers are being used as reinforcement in polymer composites for various industrial applications covering structural/non-structural and tribological usage [2-4]. Automobile sector has various applications of NFRP composites to manufacture different parts such as door panels, headliners, package trays, dashboards and interior parts of vehicle [5,6]. Other applications like sliding panels, linkage, bearing and bushing are also increasing rapidly [7]. Due to these variety of industrial and commercial applications, NFRP composites are sometimes exposed to various tribological loading conditions which forces the component under different types of wear mechanism like adhesive, abrasive and sliding wear. Therefore, it is imperative to evaluate and analyze the tribological performance of the developed composites to enhance their usability in various engineering sectors. The tribological performance (wear and friction) of NFRP composites are influenced by numerous parameters such as type of reinforcement (mat or loose fibers), treatment of fibers, orientation of fibers (parallel, anti-parallel and normal), wet and dry contact conditions and weight percentage of fibers [7,8]. Some of the previous studies reported that bio-composites achieved better wear performance under wet contact conditions as compared to dry contact condition [9,10]. Work on tribological analysis of NFRP composites has been carried out by many researchers. Authors found that reinforcing the fibers with matrix enhanced the wear performance of NFRP composites. Yousif *et al.* [11] investigated the influence of aging process on wear and frictional performance of treated oil palm/ polyester composite under dry sliding conditions with sliding distance of 0-6.72 km. Developed composites were immersed in different solutions such as water, salt water, diesel, petrol and engine oil. The results revealed that samples immersed with engine oil and diesel showed maximum wear performance due to high viscosity of engine oil and diesel. Nirmal *et al.* [12] investigated the frictional and adhesive wear performance of bamboo/epoxy composite with random, parallel and anti-parallel orientations of stacked bamboo fibers. Authors found that wear performance was superior with anti-parallel orientation of fiber and maximum frictional performance was achieved at low sliding velocity for anti-parallel orientation. Correa *et al.* [13] investigated the effect of resin, fiber size and curing agent on friction and wear behavior of musaceae/polyester composites. The research revealed that increasing the fiber size, reduced the wear resistance of the developed composites and neat polyester showed lower wear resistance as compared to musaceae/polyester composites.

*Corresponding author: vijaychaudhary111@gmail.com

Rajini *et al.* [14] reported that silane treated coconut sheath/ polyester composites filled with 2 wt% organically modified montmorillonite achieved maximum reduction in specific wear rate. Bajpai *et al.* [15] reported wear and frictional behavior of sisal /polypropylene composite under different process parameters such as applied loads (10-30 N), sliding speeds (1-3 m/s) and a constant sliding distance of 3 km. Authors concluded that incorporation of 30 wt% of sisal fiber improved wear resistance of the developed composite as compared to neat polypropylene. Jute, hemp and flax fibers belongs to the same category, that is bast fibers. Literature shows that these fibers possess promising mechanical properties [16]. It has been established that hybridization using two or more plant based fibers possesses most potential in terms of applicability [17]. Jawaid *et al.* [18] developed hybrid composites using jute/oil palm fibers and concluded that strength was improved due to hybridization. Flax reinforced polymer composite have been used in automobile and construction industry [19].

In a previous study on various hybrid composites using jute/hemp/flax reinforced epoxy composites has been concluded that tensile strength, tensile modulus and impact strength of jute/hemp/flax reinforced epoxy composite has got improved whereas flexural strength and flexural modulus of some hybrid composite has reduced [16]. Maximum wear studies available are on either on unidirectional mat or randomly oriented mat based composites. Not much research has been done on wear behavior of hybrid composites comprising three different plant fibers.

Bi-directional reinforcement offers a unique solution to ever increasing demands on the advanced materials in terms of better performance and ease in processing. As woven fabrics offer high strength and stiffness, these have been used in various structural application, aerospace, defence, automobile and wear applications [20,21]. Woven fabric offers more resistance to wear as compared to other type of orientation due to cross-linking points of woven mats. This reduces the possibility of the fiber pull-out, fiber displacement and debonding between fiber/matrix under tribological loading. Bi-directional woven mat reinforced polymer composites offer significant resistance to wear in longitudinal, transverse and normal direction of rubbing.

In various tribological applications, the friction force acting between the specimen and the counterface of tribometer generates heat because of the frictional resistance. The generated heat gets distributed between the counterface and the specimen according to the conductivity of the materials. This transferred heat to the composite, increases the temperature of the polymer composite and sometimes the temperature gets above the glass transition temperature of the polymer composite. After the glass transition temperature, the polymer composite specimen changes its physical shape, which could lead to a catastrophic failure while the composite is in operation. Dynamic mechanical analysis (DMA) predicts the behavior of polymer composites with the change in the temperature above or below the glass transition temperature of specimen. DMA enables to predict the viscoelastic behavior of polymeric composites under application of load and temperature simultaneously by detecting the glass transition temperature of the developed composite [22]. NFRP composites exhibit unique viscoelastic properties due to the combined effect of viscous properties of matrix and elastic properties of the fiber reinforcement. The viscoelastic behavior of NFRP composite under application of load varies when the temperature varies from lower to higher level. The damping capability (tanδ) is largely influenced by the interfacial adhesion of fiber/matrix interface [23].

In the present study, three types of plant based natural fibers (jute, hemp, flax) and their hybridized combinations of jute/hemp, hemp/flax and jute/hemp/flax were used in woven mat form to be reinforced with epoxy matrix. To the author's best knowledge, the wear performance of these hybrid composites have not been carried out in depth. DMA analysis of the developed composites has been performed at constant frequency of 1 Hz. Frictional and wear performance of the processed composites have been evaluated at different levels of process parameters (applied load, sliding speed and distance).

Experimental

Fibers and Matrix

Jute, Hemp and flax fibers were supplied by Compact buying services, Faridabad (India). Bi-directional woven mats of these cellulosic fibers have been used for the fabrication of bio-composites. Epoxy (resin and hardener) used as a matrix material, was supplied by Shankar Dyes and Chemicals, Delhi-06 (India). Jute, hemp and flax fiber mats along with their SEM micrographs are shown in Figure 1.

Processing

The matrix was prepared by proper mixing of epoxy resin of J3P grade and universal 10000 hardener in proportion of 2:1. Epoxy resin and hardener were properly mixed to reduce the air bubbles present in the liquid of resin and hardener. Bio-composites were fabricated with the help of detachable closed mold of mild steel using hand lay-up technique. The silica gel was applied to the inner surface of mold plates to avoid sticking of polymer with the steel plates during curing. The liquid resin was then uniformly spread on the inner surface of the mold and the resin was rolled by the steel roller to achieve the equal thickness of resin layer over the surface of the mold. Fiber mats were cut in equal size as of mold cavity and placed over the layer of resin. Roller was again rolled over to remove any air bubble trapped within the layer. This process was repeated again and again till the pre-decided specifications. For each type of developed bio-composite, the weight fraction of reinforcement was kept

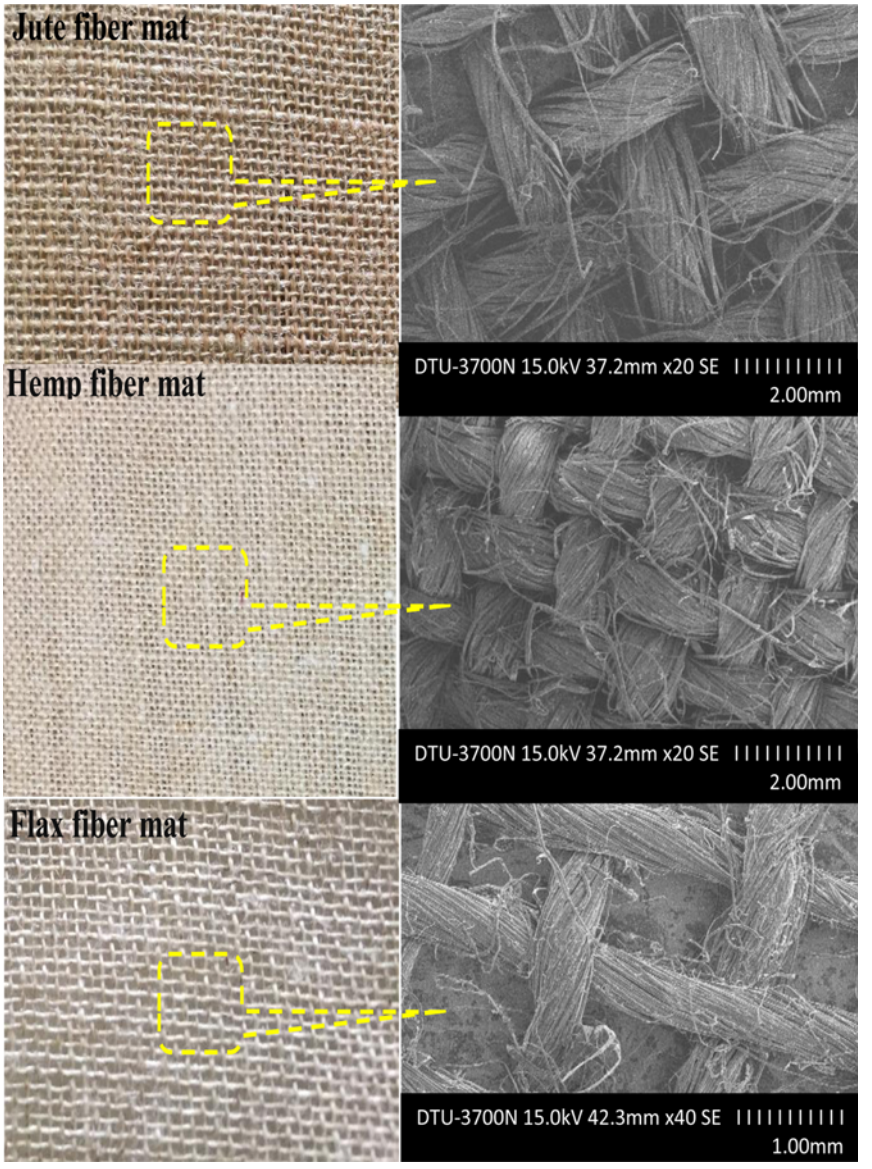

Figure 1. SEM micrographs of jute, hemp and flax fiber mat.

Table 1. Abbreviations for composites

Abbreviation	Description
J/Epoxy	Jute/epoxy
H/Epoxy	Hemp/epoxy
F/Epoxy	Flax/epoxy
J/H/Epoxy	Jute/Hemp/epoxy
H/F/Epoxy	Hemp/Flax/epoxy
J/H/F/Epoxy	Jute/Hemp/Flax/epoxy

constant to 25 %. Table 1 shows the list of abbreviations for the developed bio-composites which has been used throughout this study.

Experimental Procedure

Wear Test Set-up

Friction and wear tests were conducted on high temperature pin-on-disc tribometer (DUCOM India, TR-20LE-PHM 400). The tribometer had a counterface of hardened steel (EN-31) having hardness 64 HRC with surface roughness 0.7 mm Ra. The system records the values of frictional force at every 0.9 seconds. Tribometer also has various digital display indicators which displays the friction force, time, time/revolutions and temperature values. The specimen held in specimen holder rubes against steel counterface as the rotation starts. The dead weight is applied through a pulley system. The schematic of experimental setup is shown in Figure 2.

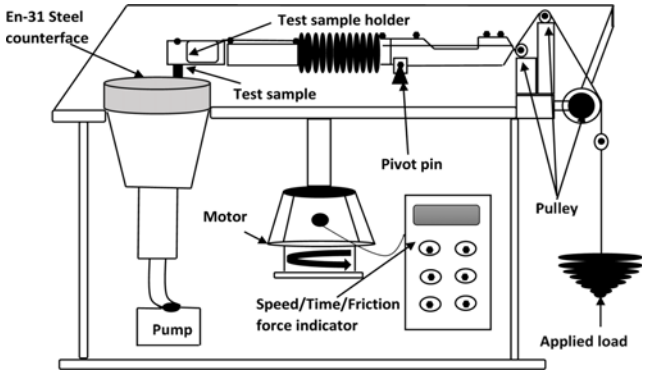

Figure 2. Schematic diagram of pin-on-disc tribometer.

Wear Testing

Specimens were prepared as per ASTM G99-95 standard. Sliding speed (1-5 m/s), applied load (10-50 N) and sliding distance (1000-2000 m) were the test conditions to evaluate frictional force and specific wear rate of the developed composites. After each experiment, the steel plate was rubbed by SiC abrasive paper, grade no.1500 to maintain the initial surface condition of steel plate. After each experimentation, the plate and specimen were cleaned by acetone with the help of cotton. The sliding direction of the bio-composite specimen is shown in Figure 3. With the help of recorded friction force, the coefficient of friction was calculated using the following relation.

$$Coefficient\ of\ friction\ (\mu) = \frac{Frictional\ force\ (F_f)}{Applied\ load\ (F_n)} \quad (1)$$

For the measurement of specific wear rate, weight of the test specimen before and after each wear experimentation was measured using an electronic balance (Shimadzu Japan, AUW. 220D) having least count of 0.001 mg. The difference between weights gives the mass of worn out material of the test sample. The following relation was used to calculate the specific wear rate of the test sample.

$$Specific\ wear\ rate\ (K_S) = \frac{Mass\ loss\ during\ test\ (m)}{Density\ (\rho) \times Applied\ load\ (F_n) \times Sliding\ distance\ (L)} \quad (2)$$

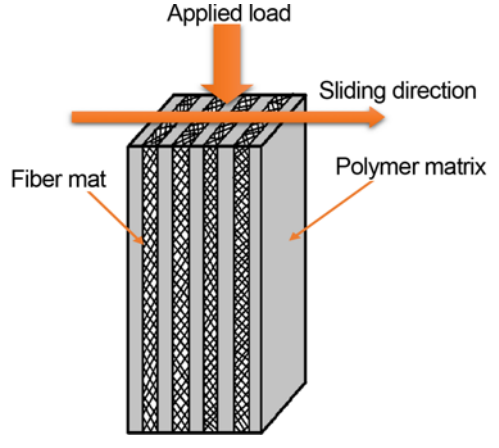

Figure 3. Schematic representation of sliding direction of composite specimen.

Dynamic Mechanical Analysis (DMA)

The DMA analyses was performed with Perkin Elmer Thermal Analyzer (DMA 8000). The equipment was operated in three bending point mode according ASTM D7028 at a frequency of 1 Hz, heating rate of 2 °C/min and with a temperature range from 0 °C to 110 °C, according ASTM D7028. The storage modulus (E'), loss modulus (E'') and damping capability (tan δ) were recorded with respect to temperature variation.

Results and Discussion

Damping Characteristics

The effect of temperature on the damping capability (tan δ) of neat epoxy, J/Epoxy, H/Epoxy, F/Epoxy, J/H/Epoxy, H/F/Epoxy and J/H/F/Epoxy composite was evaluated at constant frequency of 1 Hz as shown in Figure 4. Incorporation of natural fibers with the epoxy matrix has influenced the damping capability of the resulting composites as shown in the Figure 4 where different tan delta peaks are observed for different composites. The highest point on the tan δ curve gives the glass transition temperature of any material. The glass transition temperature at which the polymer composite starts changing from the glassy state to rubbery state can be easily detected by tan δ curve [23]. Neat epoxy achieved the highest damping capability (tan δ) of 0.81 at the glass transition temperature (T_g) of 74 °C. As the temperature increased from 0 °C to 60 °C, neat epoxy observed almost negligible change in tan δ value which implies low damping in this temperature range. However, all the developed bio-composites, except J/H/F/Epoxy composite have shown

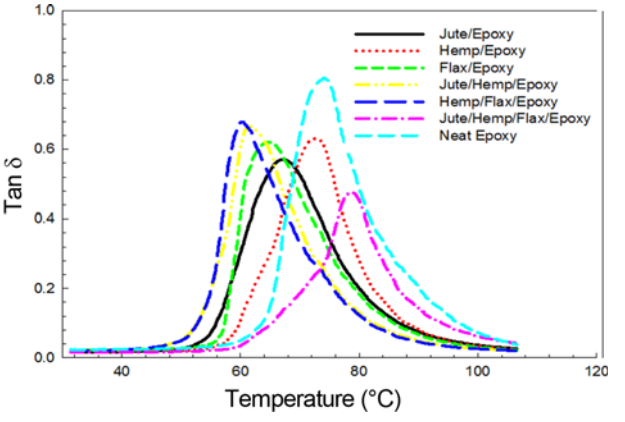

Figure 4. Damping curve of the developed composites.

fairly enhanced damping capability in this temperature range due to natural fiber reinforcement. Damping capability directly indicates the measure of elastic and non-elastic nature of any material. Higher the damping capability implies highly non-elastic components whereas high elastic nature will have low damping capability of the material [23]. In the present study epoxy has shown higher damping capability which confirms the highly brittle nature of epoxy. Due to reinforcement of various fibers, damping capability has reduced as shown in Figure 4. This means that brittleness of epoxy has reduced due to reinforcement of plant fiber. J/H/F reinforced hybrid composite has observed lowest damping capability which is indicative of highest elastic nature of the composite among all the developed composites.

As the temperature further increased from 60 °C, neat epoxy and all the developed bio-composites except J/H/F/Epoxy have reached to their maximum damping capability well before 74 °C. Thereafter, all of those have shown sharp decrease in the damping capability with increase in temperature and finally became negligible at around 100 °C. The maximum damping capability of J/H/F/Epoxy composites was recorded as 0.47 at glass transition temperature of 79 °C which was little higher (5 °C) than that of neat epoxy.

H/F/Epoxy hybrid composite achieved the second highest damping capability (tan δ) of 0.68 while it showed the minimum glass transition temperature of 60 °C. J/H/Epoxy hybrid composite showed the maximum damping capability of 0.66 at glass transition temperature of 62 °C. Other three composites i.e. J/Epoxy, H/Epoxy and F/Epoxy showed the maximum damping capability (tan δ) of 0.58, 0.62 and 0.61 respectively which were closed to each other. Hybrid composites J/H/Epoxy and H/F/Epoxy showed the improvement in the damping capability but the glass transition temperature (T_g) was reduced slightly. From the results obtained, it can be seen that glass transition temperature is the influential parameter due to the possibility of higher molecular activities at T_g in which the state of the polymer composite changes from "glassy", rigid to "rubbery" state [23].

In natural fiber based polymer composites, fiber/matrix interfacial adhesion also affects the damping capability of all the developed bio-composites. Strong interfacial adhesion between fiber/matrix interfaces restricts the movement of molecular chains of polymer and reduces the loss modulus of the composites, which further reduces the damping capability. In contrast, lower interfacial adhesion between fiber/matrix interfaces allows the movement of molecular chains of polymer and increases the loss modulus of the composites, which further increases the damping capability of the developed composites [24].

Same study was conducted for banana/polyester composites to analyze the damping factor of the developed composite. The authors concluded that incorporation of banana fiber with polyester resin reduces the damping value of the developed composites as compared to neat polyester due to elastic nature of banana fiber [25]. Chua *et al.* [26] analyzed that a polymer based composite with poor fiber/matrix adhesion produces more energy than that of the one having good fiber/matrix adhesion. Saha *et al.* [27] developed jute/polyester composites and revealed that incorporation of jute fiber with polyester resin reduced the tanδ peak height by restricting the movement of polymer molecules.

Storage Modulus (*G′*)

As shown in Figure 5, the storage modulus (*G′*) has been recorded at constant frequency of 1 Hz against the temperature for neat epoxy and each type of the developed composite. Storage modulus represents the energy stored by the composites when the load is applied. More the energy stored by the composite, more would be the value of storage modulus and hence less would be the value of damping (tan δ). If storage modulus increases, tan δ decreases [23]. From the Figure 5, it can be seen that as the temperature starts increasing, the storage modulus remains almost constant till certain range of temperature (approximately 80 % of glass transition temperature) for all the developed composites. After that, all the composites observed a drastic reduction in the value of storage modulus till glass transition temperature and finally becomes zero. This is due to the rubbery state achieved by the composites at the glass transition temperature. The dependency of the storage modulus on temperature is linear in nature. Higher the glass transition temperature of a composite, higher would be the time taken by the composite to lose its storage modulus [23].

F/Epoxy composite achieved the highest storage modulus of 1.6 GPa at room temperature which was almost two times higher than that for neat epoxy (0.8 GPa at room temperature). This may be attributed to the enhanced stiffness of the resulting composite due to the reinforcement of flax fibers to epoxy polymer at room temperature. All the developed bio-composites except F/Epoxy have shown decrement in the storage modulus as compared to neat epoxy polymer. The storage modulus recorded for J/H/F/Epoxy was 0.5 GPa at room temperature. The storage modulus recorded at room temperature for J/Epoxy, H/Epoxy, J/H/Epoxy and H/F/

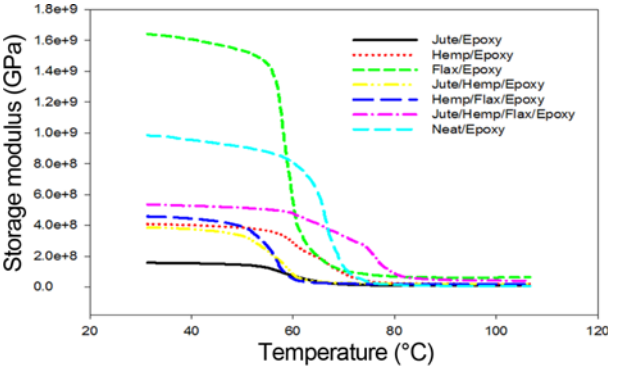

Figure 5. Storage modulus of the developed composites.

Epoxy was 0.157 GPa, 0.4 GPa, 0.37 GPa and 0.44 GPa respectively. Similar study was conducted for banana/polyester composites to analyze the storage modulus of the developed composite. Authors concluded that incorporation of banana fiber with polyester resin reduced the storage modulus of resulting composite due to dilution of polyester as compared to neat polyester [25]. In another study, the effect of cyanoethylation of jute fiber on the storage modulus of jute/polyester composite was investigated. Authors concluded that chemical treatment of jute fiber improved the wettability of fiber with resin and also improved the interfacial adhesion between fiber and matrix which increased the storage modulus of treated jute fiber reinforced polymer composites [27].

Loss Modulus (*G″*)

The loss modulus (*G″*) has been recorded at a constant frequency of 1 Hz and plotted against the temperature for neat epoxy and each type of developed composites as shown in Figure 6. The loss modulus (*G″*) spectrum for all the developed composites appears as a single peak. At the room temperature F/Epoxy composite showed the maximum value of loss modulus. As the temperature increased up to the glass transition temperature range, the loss modulus remained constant for all the developed composites. In the glass transition temperature range, the loss modulus of each composite increased to a maximum value. This increment in the loss modulus may be hypothesized due to the rubbery state of the polymer composite [23]. After the glass transition temperature range, the loss modulus of all the developed composite specimens including neat epoxy decreased sharply and finally reached to zero. The loss modulus achieved by the F/Epoxy composite in the glass transition temperature range was 0.22 GPa, which was maximum among all the developed composites. The next highest value of the loss modulus was recorded for the J/H/F/Epoxy composite of .079 GPa. The loss modulus achieved by the J/Epoxy, H/Epoxy, J/H/Epoxy and H/F/Epoxy composites were 0.024 GPa, 0.06 GPa, 0.058 GPa and 0.066 GPa respectively. Similar work for banana/polyester composites was conducted by pothan *et al.* [25] to analyze the loss modulus of the developed composite. Authors concluded that incorporation of banana fiber with polyester resin reduced the loss modulus of the developed composite due to dilution of polyester as compared to neat polyester. Saha *et al.* [27] investigated the loss modulus of jute/polyester composites and revealed that incorporation of jute fiber with polyester resin substantially affected loss modulus peak.

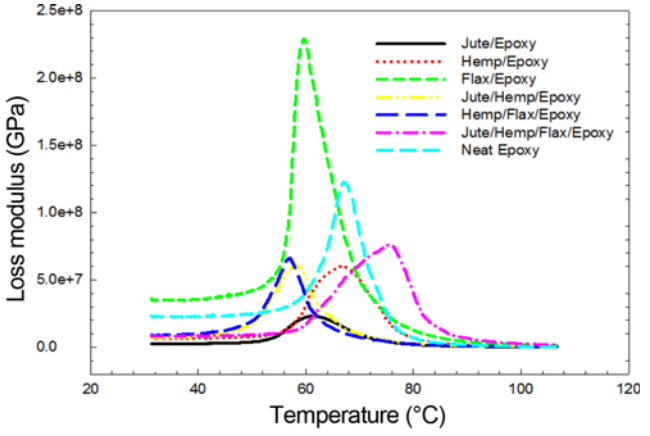

Figure 6. Loss modulus of the developed composites.

Friction Force and Coefficient

The friction force was recorded by the computer controlled tribometer for neat epoxy, J/Epoxy, H/Epoxy, F/Epoxy, J/H/Epoxy, H/F/Epoxy and J/H/F/Epoxy composites after every 100 second repeatedly as shown in Figures 7-9. Experiments for friction force were performed at the applied load of (10 N to 50 N), sliding speed of (1, 3, and 5 m/s) and time of sliding as (16 min, 24 min, and 32 min). The friction force was plotted against the sliding time for all types of the developed composites at different loads for a constant speed of 3 m/s. Increment in the applied load from 10 N to 50 N showed the increasing trends in the frictional force for all the developed composites. At the load of 10 N and sliding speed of 3 m/s, J/Epoxy achieved the maximum friction force of 7.17 N. The friction force recorded for H/Epoxy composite and J/H/Epoxy was 5.05 N and 7 N respectively. The friction force achieved by J/H/F/Epoxy, H/F/Epoxy and F/Epoxy was 4.78 N, 4.66 N and 4.49 N respectively, which were very close to the friction force of neat epoxy (4.42 N) at 10 N load. At the load of 30 N and sliding speed of 3 m/s, J/Epoxy achieved the maximum friction force of 27.17 N as compared to the friction force of neat epoxy (12.87 N). The friction force recorded for H/Epoxy composite and J/H/Epoxy was 22.67 N and 25.64 N respectively. The friction force achieved by J/H/F/epoxy, H/F/epoxy and F/Epoxy was 22.13 N, 21.15 N and 14.61 N respectively. At the load of 50 N and sliding speed of 3 m/s, J/Epoxy achieved the maximum friction force of 28.4 N as compared to friction force of 20.4 N for neat epoxy. The friction force recorded for H/Epoxy composite and J/H/Epoxy was 26.88 N and 27.01 N respectively. The friction force achieved by J/H/F/Epoxy, H/F/Epoxy and F/Epoxy was 24.32 N, 23.73 N and 21.27 N respectively. In all the developed composites, J/Epoxy composite achieved maximum friction force. Due to rough surface of jute fiber and better wettability with epoxy resin increased the interfacial bonding between fiber/matrix interfaces of J/Epoxy composite [28]. Incorporation of jute fiber also increased the frictional force of J/H/Epoxy and J/H/F/Epoxy hybrid composites as compared to H/Epoxy and F/Epoxy composites.

In Figures 10-12, the coefficient of friction (COF) has been plotted against varying applied load at different sliding speeds of 1 m/s, 3 m/s and 5 m/s. At 1 m/s speed, the COF

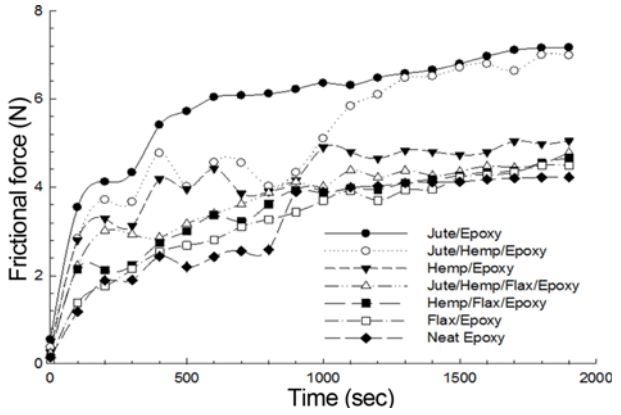

Figure 7. Frictional force at 10 N load and 3 m/s sliding speed.

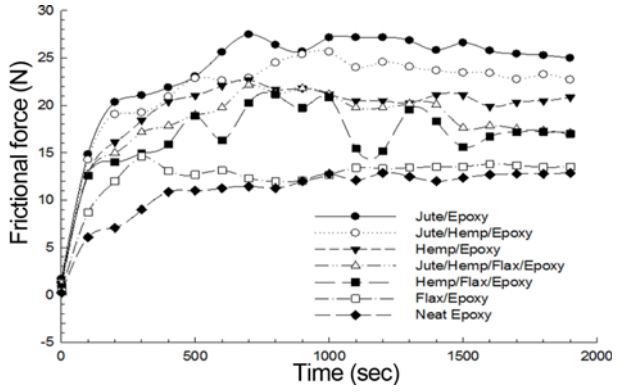

Figure 8. Frictional force at 30 N load and 3 m/s sliding speed.

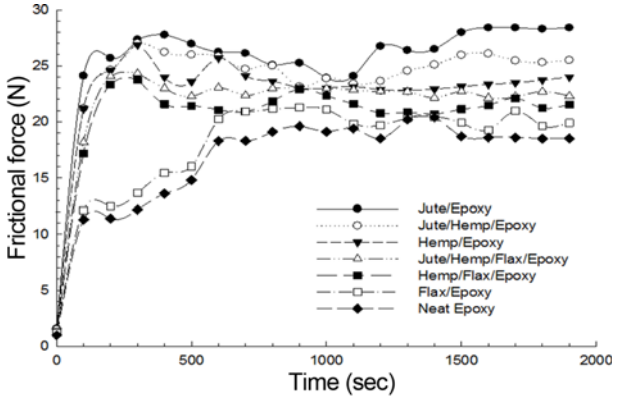

Figure 9. Frictional force at 50 N load and 3 m/s sliding speed.

increased up to 30 N load and then a small decrement was shown by all the developed composites except for neat epoxy and F/Epoxy composite. At 1 m/s sliding speed, the highest COF of 0.744 was recorded for J/Epoxy composite at 30 N load as compared to COF of neat epoxy (0.327). At 1 m/s sliding speed and 30 N load, J/H/Epoxy, H/Epoxy, J/H/F/Epoxy, H/F/Epoxy and F/Epoxy showed COF of 0.627, 0.619, 0.604, 0.504 and 0.392 respectively. As the sliding speed increased from 1 m/s to 3 m/s, the COF increased for

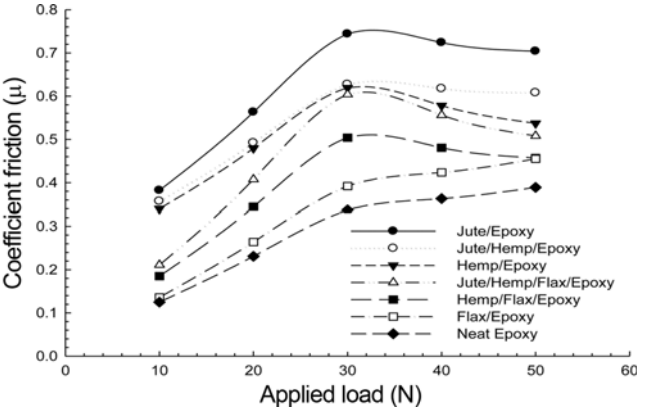

Figure 10. Coefficient of friction at 1 m/s sliding speed.

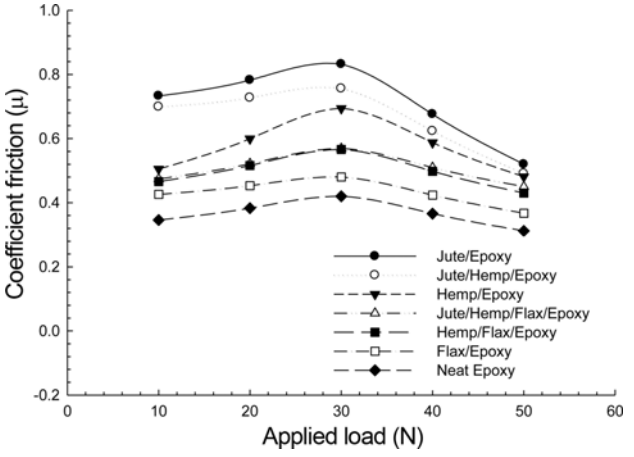

Figure 11. Coefficient of friction at 3 m/s sliding speed.

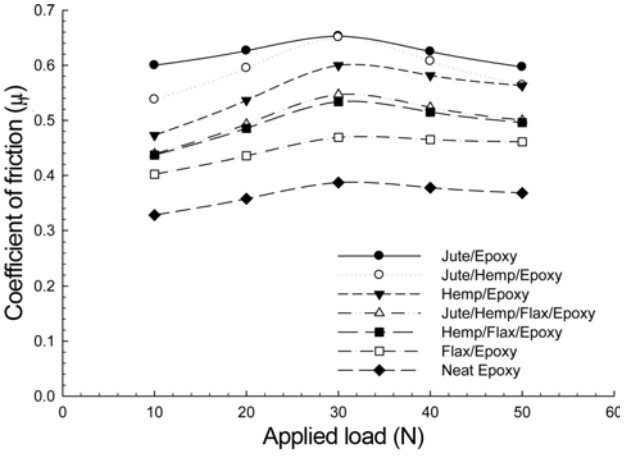

Figure 12. Coefficient of friction at 5 m/s sliding speed.

all types of the developed composites. Ahmed *et al.* [28] found similar results for J/Epoxy composite. Authors found that the developed composite showed increasing values of COF with increase in applied load (30-50 N) and sliding speed (3-6 m/s). Similar results were reported by Hashmi *et*

al. [29] in their study. Authors revealed that COF of neat polyester and cotton/polyester composite increased as applied load increased and cotton/polyester composite achieved higher COF as compared to neat polyester. At 3 m/s speed, the COF increased upto 30 N load and then a decrement was shown by all the developed composites. At 3 m/s sliding speed, the highest COF of 0.832 for J/Epoxy composite was recorded at 30 N load as compared to COF of neat epoxy (0.42). At 3 m/s sliding speed and 30 N load, J/H/Epoxy, H/Epoxy, J/H/F/Epoxy, H/F/Epoxy and F/Epoxy showed the COF of 0.756, 0.694, 0.569, 0.566 and 0.48 respectively. As the sliding speed changed from 3 m/s to 5 m/s, the COF decreased for all types of the developed composites. At 5 m/s speed, the COF increased up to 30 N load and then a decrement was shown by all the developed composites. At 5 m/s sliding speed, the highest COF of 0.653 for J/Epoxy composite was recorded at 30 N load as compared to COF of neat epoxy which was 0.387. At 5 m/s sliding speed and 30 N load, J/H/Epoxy, H/Epoxy, J/H/F/Epoxy, H/F/Epoxy and F/Epoxy showed the COF of 0.651, 0.6, 0.547, 0.534 and 0.489 respectively. COF first increased as the load increased from 10 N to 30 N and with further increment in load from 30 N to 50 N, the coefficient of friction decreased. When epoxy polymer comes in the contact of heat which was generated during the rubbing action of composite with steel counterface, it gets softened due to thermal action. At 30 N load, the temperature (25-35 ^{o}C) at the contact surface between specimen and steel counterface was not too high to lose the brittle nature of epoxy. The fiber contact with steel counterface plays a major role in increasing the COF. As the load further increased to 50 N, the role of temperature dominates the role of fiber in contact to influence the COF. At higher load of 50 N, the temperature at the contact surface between specimen and steel counterface increased upto 60 to 80 ^{o}C, which is almost equal to glass transition temperature of the developed composites. At this high temperature, thermal softening of epoxy makes an intermediate layer between specimen and sliding counterface which prevent the fibers to come in contact with the steel counterface [12]. Absence of fiber contact with the sliding counterface decreased the COF, as only the smooth and glassy layer of epoxy is in contact. Friction force and hence COF depends on interaction between composite rubbing surface and counterface. It has been established that adhesion and deformation are prevailing mechanism governing friction. Deformation is dominating on rough surface while adhesion has its impact on smooth surface [30,31]. In the present study, during experimentation it was observed that rubbing surface of composite specimen became smooth after some time of sliding. This was due to accumulation of thin film of polymer on rubbing surface of composite. This deposition of polymer film was responsible for reducing COF after some time of rubbing. Also asperities on the sliding surface of composites deform during sliding which reduces COF and finally reaches to a constant level. Fluctuations in COF may be attributed to the fact that deposited polymer film on composite sliding surface breaks and transfers to the counter surface. This again comes back or new film forms [12,32].

Specific Wear Rate

The specific wear rate has been plotted against the applied load for all types of the developed composites at different sliding speeds (1, 3 and 5 m/s) for a constant distance of 2000 m. Figure 13-15 shows that the specific wear rate (SWR) increased with increment in sliding speed for all the developed composites. First, the SWR decreased as the load changes from 10 N to 30 N, while the SWR increased or became constant as the load changes from 30 N to 50 N at all the sliding speeds. This implies that weight loss is very less till 30 N of applied load. After 30 N, weight loss has increased relatively at a faster rate with increase in applied load. Neat epoxy achieved highest SWR at all operating conditions of load, sliding speed and sliding distance. Epoxy

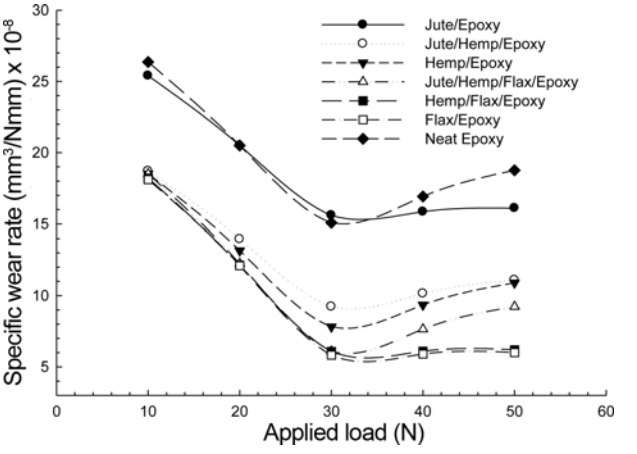

Figure 13. Specific wear rate versus applied load at 1 m/s sliding speed.

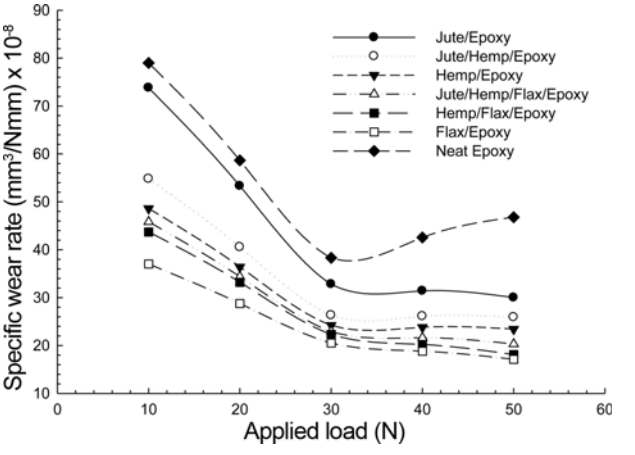

Figure 14. Specific wear rate versus applied load at 3 m/s sliding speed.

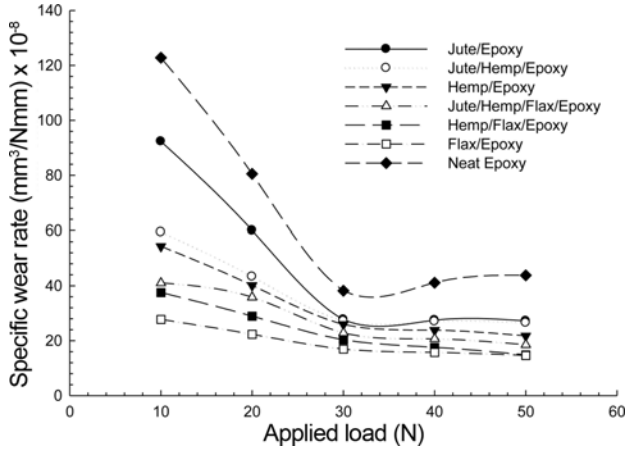

Figure 15. Specific wear rate versus applied load at 5 m/s sliding speed.

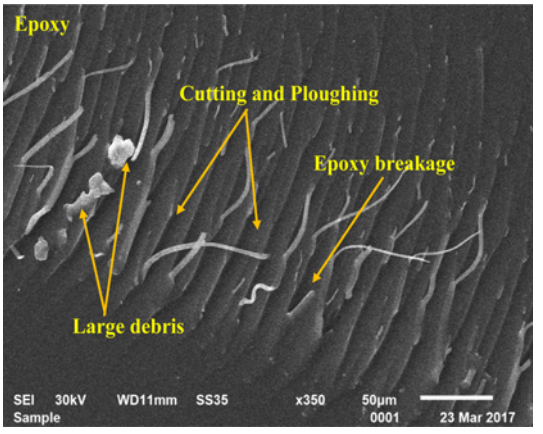

Figure 16. SEM micrographs of Epoxy for 2000 m sliding distance at 3 m/s sliding velocity and 50 N applied load.

polymer is brittle in nature and breakage or fracture of epoxy can easily be analyzed by SEM micrograph as shown in Figure 16. Incorporation of natural fibers enhanced the wear resistance of all the developed composites. In the presence of fiber mat into epoxy resin, both fiber mat and polymer participate during rubbing in wear experimentation. In such case fiber mat supports the polymer matrix from being detached by sharing the applied load. Bonding level at the fiber-matrix interface would be responsible to decide the wear of developed composite. Strong interface implies applied load during sliding would be smoothly handled by the reinforcement which in turn will increase the resistance to wear of composite surface [7]. In earlier studies, it was reported that increase in sliding velocity and load increases the SWR [33-35]. At 10 N applied load and 1m/s sliding speed, neat epoxy achieved the highest SWR of 26.36 E^{-8} mm^3/N-mm as compared to minimum SWR of 18.1 E^{-8} mm^3/N-mm for F/Epoxy composite as shown in Figure 13. As the load increased from 10 N to 30 N, SWR decreased but further increment in the load from 30 N to 50 N, the SWR of neat epoxy increased. J/Epoxy, J/H/Epoxy, H/Epoxy, J/H/F/Epoxy, and H/F/Epoxy achieved SWR of 25.4 E^{-8} mm^3/N-mm, 18.7 E^{-8} mm^3/N-mm, 18.5 E^{-8} mm^3/N-mm, 18.5 E^{-8} mm^3/N-mm, and 18.2 E^{-8} mm^3/N-mm respectively at 10 N load and 1 m/s sliding speed. From the mechanical properties of these composites reported elsewhere [36], it was found that there was substantial difference in the properties of various combinations of the developed composites. This would certainly affect the wear performance of these composites. These variations are due to variation in properties, constituents of different natural fibers, their interaction and compatibility with epoxy polymer matrix. As shown in Figure 14, at 3 m/s sliding speed and load of 10 N, neat epoxy achieved highest SWR of 79 E^{-8} mm^3/N-mm as compared to minimum SWR 37 E^{-8} mm^3/N-mm of F/epoxy composite. As the load increased from 10 N to 30 N, SWR decreased but increased with further increase in the load from 30 N to 50 N at 3 m/s sliding speed. J/Epoxy, J/H/Epoxy, H/Epoxy, J/H/F/Epoxy, and H/F/Epoxy achieved SWR of 73.8 E^{-8} mm^3/N-mm 54.8 E^{-8} mm^3/N-mm, 48.6 E^{-8} mm^3/N-mm, 45.8 E^{-8} mm^3/N-mm, and 43.7 E^{-8} mm^3/N-mm respectively. At 5 m/s sliding speed and applied load of 10N, neat epoxy achieved highest SWR of 122.8 E^{-8} mm^3/N-mm as compared to minimum SWR of 27.7 E^{-8} mm^3/N-mm of F/Epoxy as shown in Figure 15. As the load increased from 10 N to 30 N, SWR decreased but further increment in the load from 30 N to 50 N at 5 m/s sliding speed, increased the SWR of neat epoxy. J/Epoxy, J/H/Epoxy, H/Epoxy, J/H/F/Epoxy, and H/F/Epoxy achieved SWR of 92.3 E^{-8} mm^3/N-mm, 59.4 E^{-8} mm^3/N-mm, 54.3 E^{-8} mm^3/N-mm, 41 E^{-8} mm^3/N-mm, and 37.5 E^{-8} mm^3/N-mm respectively. Wear mechanism of bi-directional woven fiber mat reinforced composites can be explained by considering wear of the transverse fibers which are at 0 degree with respect to steel plate and longitudinal fibers which are at 90 degree to the steel plate as represented by the Figure 17(a). Wear of transverse fibers may happen in either of the following two ways. First, the whole fiber comes out of the composite at once. It may occur due the fact that at high temperature the bonding strength of fiber and matrix becomes lower. Second, at lower temperatures, when the bonding strength of fiber and matrix is maintained then the lower portion of the transverse fiber worn out due to the sliding action as shown in Figure 17(b) [4]. Wear of the longitudinal fibers may occur in either of the following three ways.

(a) Breaking of the fiber from the lower end into small pieces simply due to the rubbing action between the counter surface plate and the fiber in contact as shown in Figure 17(c).

(b) Fiber pull-out from the matrix as a result of excessive tangential frictional force between the counter surface plate and the fiber and the softening of the matrix material at elevated temperatures.

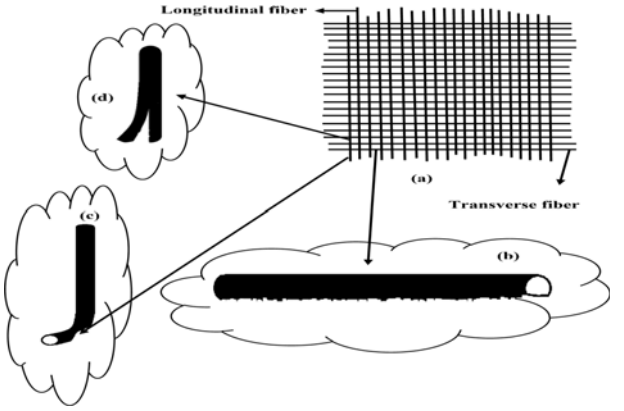

Figure 17. Schematic representation of wear mechanism.

(c) Tearing of the fiber in the direction of fiber length as shown in Figure 17(d).

Yousif and Chin [33] also reported in their study that SWR of kenaf fiber reinforced epoxy composite was increased as the load increased from 30 to 200 N. For all the developed composites, the SWR increased as the sliding speed increased from 1 m/s to 3 m/s. Similar results were shown by Ahmed *et al.* [28] for J/Epoxy composite that SWR increased as the sliding speed increased from 3 m/s to 6 m/s. Nasir *et al.* [34] developed epoxy resin impregnated gunny (jute) (RIG) and epoxy resin reinforced honeycomb (RIG) composites and investigated wear characteristics of the developed composites. Authors found that SWR of RIG increased as sliding velocity increased from 1.12 to 22.56 m/s but SWR decreased as the applied load increased.

At higher load and higher sliding speed, temperature of steel counterface of wear tribometer increased due to continuous friction between specimen and steel counterface which in turn increased the temperature of specimen resulting in thermal gradient. Some of the specimens got bend at lower end due to continuous rubbing and temperature generation at the lower end of specimen. Figure 18 shows the condition of counter steel surface after experimentation and bend specimens.

Figure 19 shows the effect of applied load (10-30 N) on the interface temperature of J/Epoxy, H/epoxy, F/epoxy, J/H/Epoxy, H/F/Epoxy and J/H/F/Epoxy composites at constant sliding speed of 5 m/s. As shown in Table 2, J/Epoxy composite achieved maximum interface temperature of 10 °C, 25 °C and 60 °C at 10, 30 and 50 N of applied load as compared to neat epoxy which achieved maximum interface temperature of 5 °C, 15 °C, 50 °C at the same operating conditions. Coefficient of friction largely influenced the interfacial temperature of all the composite specimen during wear analysis. Due to high coefficient of friction, J/Epoxy composite achieved highest interfacial temperature as compared to minimum interfacial temperature of neat epoxy which has lowest coefficient of friction. Low coefficient of friction of F/Epoxy composite is due to smother surface of flax fibers which showed lower interfacial temperature among all the

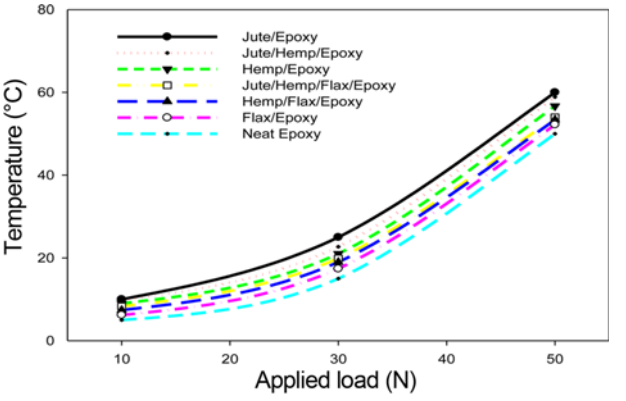

Figure 19. Temperature at interface at constant sliding speed of 5 m/s.

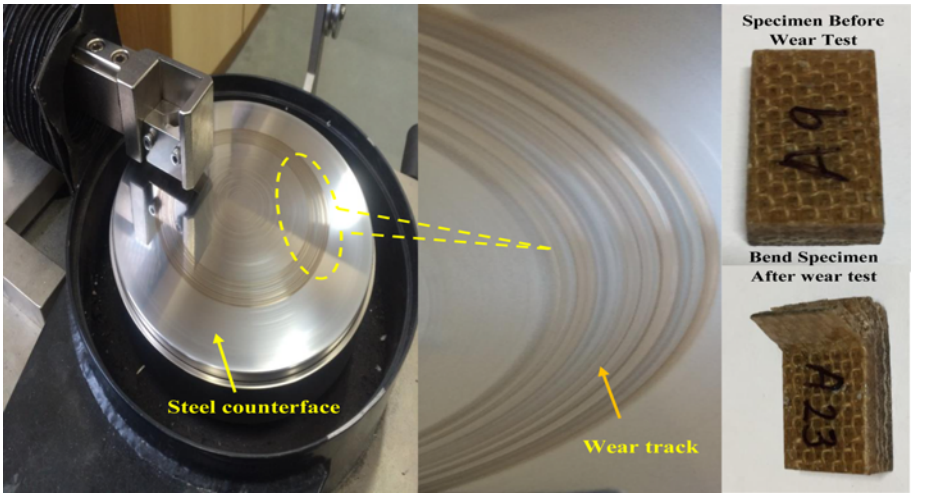

Figure 18. Wear track of steel counterface of tribometer and bend specimen.

Table 2. Temperature profile at interface during tribological analysis

Material	Maximum Temperature (°C) at 5 m/s sliding speed		
	10 N load	30 N load	50 N load
J/Epoxy	10.0	25.0	60.0
J/H/Epoxy	9.80	22.7	58.9
H/Epoxy	9.0	21.0	56.7
J/H/F/Epoxy	8.3	19.9	54.0
H/F/Epoxy	7.4	19.0	53.4
F/Epoxy	6.2	17.4	52.2
Neat Epoxy	5.0	15.0	50.0

developed composites as shown in Table 2. Chin and Yousif [36] developed kenaf/epoxy composite using a closed mould technique associated with vacuum system. Sliding wear and frictional behavior of the composite were investigated and also analyzed the effect of applied load on the generation of interfacial temperature at contact surface of the composite specimens. The author concluded that composite showing highest coefficient of friction at 5 km distance achieved maximum interfacial temperature.

The SEM micrographs of J/Epoxy, H/Epoxy, F/Epoxy and their hybrid composites (J/H/Epoxy, H/F/Epoxy and J/H/F/Epoxy) are shown in Figure 20(a-c) and Figure 21(a-c). J/Epoxy composite which achieved maximum specific wear rate can be justified by SEM micrograph at 3 m/s sliding speed and 50 N load. At higher load, fiber pull-out is clearly seen in the SEM micrograph of J/Epoxy composite.

Chin and Yousif [36] reported that the increase in load showed the debonding of fiber due to thermo-mechanical loading which weakened the fiber/matrix interfacial bonding and enhanced the material removal from the polymer matrix. SEM images of F/Epoxy composite showed minimum matrix breakage, debonding, fiber fracture and fiber pull-out

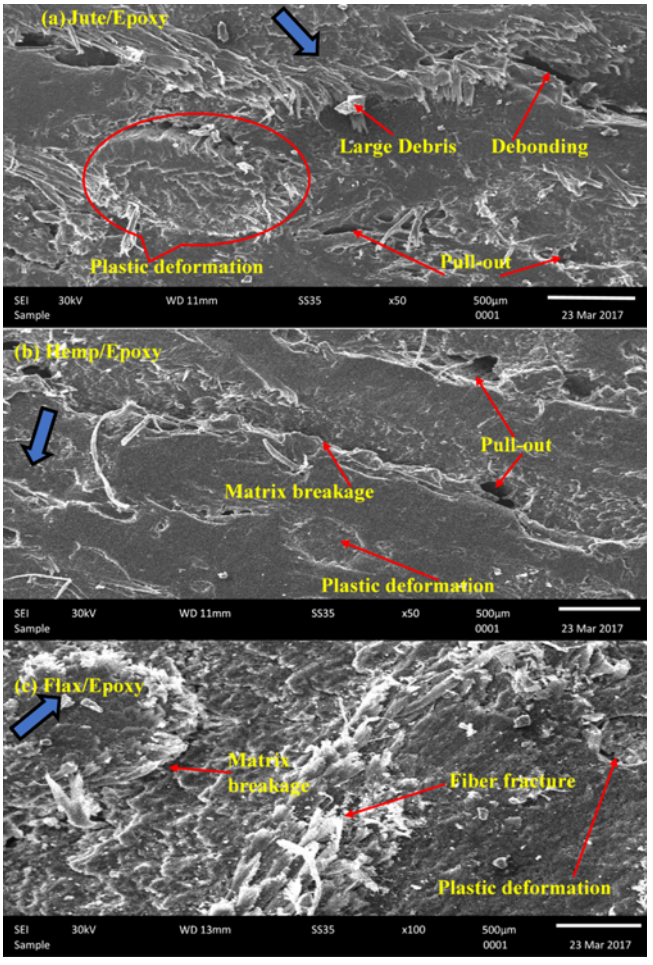

Figure 20. SEM micrographs of (a) J/Epoxy (b) H/Epoxy (c) F/Epoxy composite for 2000 m sliding distance at 3 m/s sliding velocity and 50 N applied load.

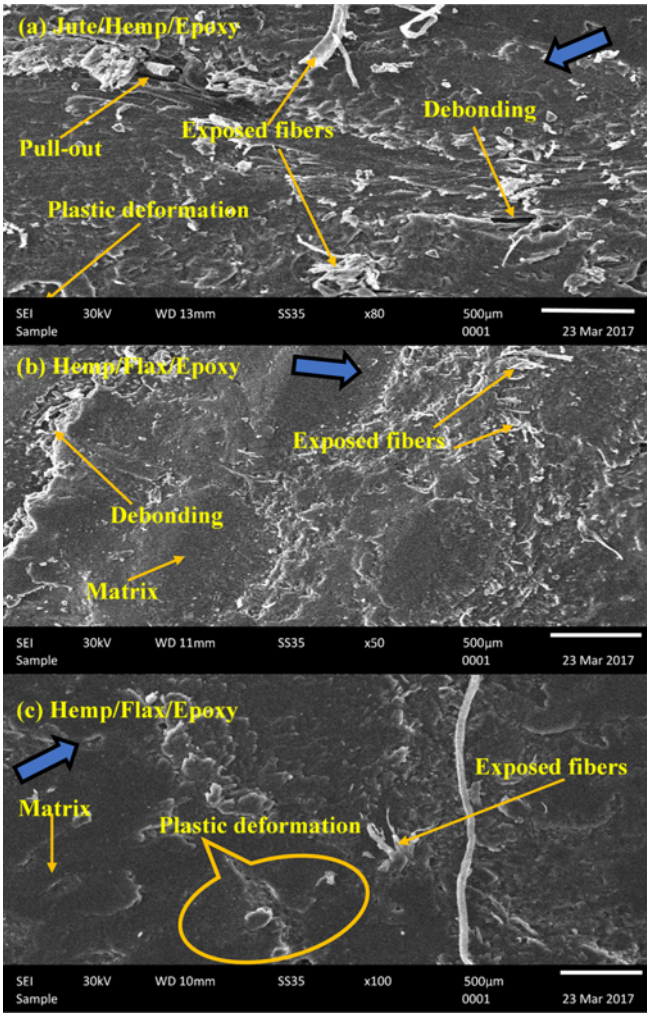

Figure 21. SEM micrographs of (a) J/H/Epoxy (b) H/F/Epoxy (c) J/H/F/Epoxy composite for 2000 m sliding distance at 3 m/s sliding velocity and 50 N applied load.

which in turn resulted in lowest SWR among the developed composites. Microscopic observation showed that H/Epoxy composite specimen after wear testing showed micro cracking, debonding of fiber and matrix breakage due to brittle nature of hemp fibers. Jute and hemp fibers formed relatively brittle composite due to the brittle nature of jute and hemp fibers but flax fibers are soft and ductile in nature. Due to this, F/Epoxy composite showed low matrix breakage, fiber fracture and debris were very less appeared in the SEM micrographs of F/Epoxy composite. At higher load of 50 N, fiber detachment and fiber pull-out were hardly observed in SEM image of F/Epoxy composite. In hybrid composites, J/H/Epoxy composite achieved maximum specific wear rate. Matrix cracking, debonding and fiber fracture can be clearly seen in the SEM micrograph of J/H/Epoxy composite. Fiber pull-out, matrix breakage and debris formation were less observed in SEM micrographs of J/H/F/Epoxy composite worm surface and fibers were still in good condition. In H/F/Epoxy composite, the worn surface showed substantial amount of fiber debonding and fiber fracture.

Conclusion

In the present work, dynamic mechanical analysis and tribological performance of natural fiber reinforced epoxy composites were analyzed and the morphology of worm out surfaces of wear specimens were examined using SEM.

The following points can be concluded from the present findings:

1. Incorporation of natural fibers (jute, hemp and flax) with epoxy polymer has enhanced the wear resistance of all the developed composites.
2. The effect of speed is nominal on coefficient of friction at higher speed whereas applied load has negligible effect on coefficient of friction. Average coefficient of friction is different for each type of composite. This concludes that type of natural fiber affects the friction conditions on the developed composites.
3. Reinforcement of different combination of natural fibers has substantially enhanced the wear performance of epoxy. Sliding speed has significant effect on wear performance of the developed composites along with the applied loads.
4. Jute/hemp hybrid composite has shown better wear performance as compared to other combinations of hybrid composites.
5. Analysis of interfacial temperature during wear shows that as the applied load increases, temperature at interface continuously increases.
6. Debonding, fiber pull-out and tearing of fibers were the major factors for wear of the developed composites as depicted by SEM micrographs. Plastic deformation and ploughing action established abrasive and adhesive type of wear mechanism.
7. Dynamic mechanical analysis of the developed composites shows that reinforcement of natural fibers has markedly improved the thermal stability of neat epoxy under dynamic loading conditions. Results conclude that dynamic mechanical characteristics (damping capability, storage and loss modulus) have a great dependency on the type of natural fibers and its hybrid combinations reinforced with epoxy polymer.
8. Results of damping capability has shown that incorporation of natural fibers has reduced the brittle nature of epoxy matrix to a greater extent.

References

1. F. M. AL-Oqla, S. M. Sapuan, M. R. Ishak, and A. A. Nuraini, *Fiber. Polym*., **16**, 153 (2015).
2. I. O. Oladele and N. I. Agbeboh, *Fiber. Polym*., **18**, 1336 (2017).
3. A. M. Radzi, S. M. Sapuan, M. Jawaid, and M. R. Mansor, *Fiber. Polym*., **18**, 1353 (2017).
4. A. Balaji, B. Karthikeyan, J. Swaminathan, and C. S. Raj, *Fiber. Polym*., **18**, 1193 (2017).
5. C. Alves, P. M. C. Ferrao, A. J. Silva, L. G. Reis, M. Freitas, L. B. Rodrigues, and D. E. Alves, *J. Clean Prod.*, **18**, 313 (2010).
6. J. Holbery and D. Houston, *JOM*, **58**, 80 (2006).
7. P. K. Bajpai, I. Singh, and J. Madaan, *Wear*, **297**, 829 (2013).
8. N. S. M. El-Tayeb, B. F. Yousif, and T. C. Yap, *Tribol Int.*, **41**, 331 (2008).
9. A. Borruto, G. Crivellone, and F. Marani, *Wear*, **222**, 57 (1998).
10. J. Wu and X. H. Cheng, *Wear*, **261**, 1293 (2006).
11. B. F. Yousif and U. Nirmal, *Wear*, **272**, 97 (2011).
12. U. Nirmal, J. Hashim, and K. O. Low, *Tribol Int.*, **47**, 122 (2012).
13. C. E. Correa, S. Betancourt, A. Vazquez, and P. Ganan, *Tribol Int.*, **87**, 57 (2015).
14. N. Rajini, J. T. W. Jappes, B. Suresha, S. Rajakarunakaran, I. Siva, and N. Azhagesan, *Proc. Inst. Mech. Eng. PartJ*, **228**, 483 (2014).
15. P. K. Bajpai, I. Singh, and J. Madaan, *Proc. Inst. Mech. Eng. PartJ: J. Eng. Tribol.,* **227**, 385 (2013).
16. V. Chaudhary, P. K. Bajpai, and S. Maheshwari, *J. Nat. Fibers*, doi:10.1080/15440478.2017.1320260 (2017).
17. S. N. A. Safri, M. T. H. Sultan, M. Jawaid, and K. Jayakrishna, *Compos. Pt. B-Eng*., doi:10.1016/j.compositesb.2017.09.008 (2017).
18. M. Jawaid, O. Y. Alothman, M. T. Paridah, and H. S. P. A. Khalil, *Int. J. Polym. Anal. Charact.,* **19**, 62 (2014).
19. V. Fiore, T. Scalici, L. Calabrese, A. Valenza, and E. Proverbio, *Compos. Pt. B-Eng*., **84**, 258 (2016).
20. B. F. Yousif and N. S. M. EI-Tayeb, *Wear*, **265**, 856 (2008).
21. J. P. Davim and C. Rosaria, *Wear*, **266**, 795 (2009).
22. M. Lahelin, I. Aaltio, O. Heczko, O. Soderberg, Y. Ge, B.

Lofgren, S. P. Hannula, and J. Seppala, *Compos. Pt. A-Appl. Sci. Manuf.*, **40**, 125 (2009).
23. N. Saba, M. Jawaid, O. Y. Alothman, and M. T. Paridah, *Constr Build Mater.*, **106**, 149 (2016).
24. V. G. Geethamma, G. Kalaprasad, G. Groeninck, and S. Thomas, *Compos. Pt. A-Appl. Sci. Manuf.*, **36**, 1499 (2005).
25. L. A. Pothan, Z. Oommen, and S. Thomas, *Compos. Sci. Technol.*, **63**, 283 (2003).
26. T. Murayama, "Dynamic Mechanical Analysis of Polymeric Material", 2nd ed., Elsevier, New York, 1982.
27. A. K. Saha, S. Das, D. Bhatta, and B. C. Mitra, *J. Appl. Polym. Sci*., **71**, 1505 (1999).
28. K. S. Ahmed, S. S. Khalid, V. Mallinatha, and S. J. Amith Kumar, *Mater. Des.*, **36**, 306 (2012).
29. S. A. R. Hashmi, U. K. Dwivedi, and N. Chand, *Wear*, **262**, 26 (2007).
30. N. S. M. EI-Tayeb, *Wear*, **265**, 223 (2008).
31. L. Zsidai, P. De Baets, P. Samyn, G. Kalacska, A. P. Van Peteghem, and F. V. Parys, *Int. J. Wear*, **253**, 675 (2002).
32. K. L. Edwards, *Mater. Des.*, **19**, 1 (1998).
33. B. F. Yousif and C. W. Chin, *Surf. Rev. Lett.*, **19**, 1250050 (2012).
34. R. M. Nasir, M. R. A. Montaha, V. Radha, V. Radha, A. Y. Saad, and H. W. Gitano-Briggs, *Mater Des.*, **48**, 34 (2013).
35. B. F. Yousif and N. S. M. El-Tayeb, *Tribol Lett.*, **32**, 199 (2008).
36. C. W. Chin and B. F. Yousif, *Wear*, **267**, 1550 (2000).